



Contents lists available at ScienceDirect

Bioorganic & Medicinal Chemistry

journal homepage: www.elsevier.com/locate/bmc

Mycophenolic acid analogs with a modified metabolic profile

Liqliang Chen^{a,*}, Daniel J. Wilson^a, Nicholas P. Labello^a, Hiremagalur N. Jayaram^b, Krzysztof W. Pankiewicz^a

^aCenter for Drug Design, Academic Health Center, University of Minnesota, 516 Delaware Street S.E., Minneapolis, MN 55455, USA

^bDepartment of Biochemistry and Molecular Biology, Indiana University School of Medicine and Richard Roudebush Veterans Affairs Medical Center, 1481 West Tenth Street, Indianapolis, IN 46202, USA

ARTICLE INFO

Article history:

Received 14 July 2008

Revised 20 August 2008

Accepted 26 August 2008

Available online 29 August 2008

Keywords:

Mycophenolic acid

Inosine monophosphate dehydrogenase

Allylic substitution

ABSTRACT

Mycophenolic acid (MPA), a clinically used immunosuppressant, is extensively metabolized into an inactive C7-glucuronide and removed from circulation. To circumvent the metabolic liability imposed by the C7-hydroxyl group, we have designed a series of hybrid MPA analogs based on the pharmacophores present in MPA and new generations of inosine monophosphate dehydrogenase (IMPDH) inhibitors. The synthesis of MPA analogs has been accomplished by an allylic substitution of a common lactone. Biological evaluations of these analogs and a preliminary structure–activity relationship (SAR) are presented.

© 2008 Elsevier Ltd. All rights reserved.

1. Introduction

Mycophenolic acid (Fig. 1, MPA), arguably the first antibiotic, was isolated more than one hundred years ago.¹ Subsequent studies revealed the role of MPA as a highly potent inhibitor of inosine monophosphate dehydrogenase (IMPDH), a key enzyme in the de novo synthesis of guanine nucleotide. Consequently, MPA exhibits an impressive anti-proliferation activity and has been established as an anti-cancer² and anti-viral agent, as well as an immunosuppressant.³ Currently mycophenolate mofetil (Fig. 1, MMF, a pro-drug of MPA) and mycophenolate sodium (MPS) are used in combination with other immunosuppressants for the treatment of organ rejection in heart, liver, and kidney transplants.

While it is widely used in transplantation, MPAs anti-cancer properties are again of current interest. For instance, MPA has been demonstrated to be an effective inducer of differentiation in a number of cancer cell lines such as those of androgen-independent prostate cancer,^{4,5} leukemia,⁶ and melanoma.⁷ A more recent study showed that MPA exerted its anti-angiogenic effect through inhibition of human IMPDH type 1,⁸ an isoform long believed to be a house keeping enzyme. Furthermore, MPA acts synergistically with imatinib,⁹ a first line therapy in the treatment of chronic myelogenous leukemia (CML). These findings strongly support the role of MPA as a potential anti-cancer agent.

In addition to its anti-cancer activity, MPA has also been subjected to structural modifications that elicit interesting biological properties other than inhibition of IMPDH. A recent study revealed

that mycophenolic acid and its close analogs behaved as agonists of peroxisome proliferator activated receptor γ (PPAR γ).¹⁰ Furthermore, we designed a hybrid compound, in which the carboxylic acid of MPA was replaced with a hydroxamic acid group. This minor structural modification converted MPA into mycophenolic acid hydroxamic acid (Fig. 1, MAHA),¹¹ a dual inhibitor of both IMPDH and histone deacetylases (HDAC). These studies confirmed versatile biological properties of MPA and the significance of MPA core structure as a potentially useful pharmacophore.

Unfortunately, mycophenolic acid suffers from a severe metabolic drawback. The C7-phenolic hydroxyl group is highly susceptible to glucuronidation, which abrogates its inhibitory activity against IMPDH. This metabolic liability might explain the limited clinical efficacy of MPA as demonstrated in a Phase I clinical trial of mycophenolate mofetil in advanced multiple myeloma patients.¹² Furthermore, subsequent cleavage of MPA glucuronide in the gastrointestinal track causes side effects and also leads to secondary absorption peaks through a process called enterohepatic recirculation.¹³

Consequently, MPA analogs and mimics that lack MPAs metabolic liability have been pursued by researchers in both academia and industry. Significant efforts were focused on bio-isosteric replacements, albeit with limited success. For instance, replace-

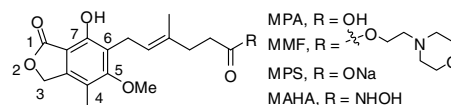


Figure 1. Mycophenolic acid and its derivatives.

* Corresponding author. Tel.: +1 612 625 3264; fax: +1 612 624 8252.
 E-mail address: chenx462@umn.edu (L. Chen).

ment of 7-hydroxyl group with a fluorine atom drastically reduced the inhibitory activity.¹⁴ A C7-amino analog of MPA was resistant to glucuronidation, however with significantly reduced anti-IMPDPH inhibitory activity.¹⁴ In yet another isosteric replacement, the phenolic hydroxyl group was replaced with an indole NH group, resulting in a MPA analog with a low micromolar mean GI₅₀ in a NCI human tumor panel screen.¹⁵ However, further modification by introducing a methyl and methoxy group, both of which were believed to favorably position the hexenoic side chain in MPA, produced an inactive compound.¹⁶

Our group designed MPA derivatives in which a truncated MPA was connected to an adenosine moiety via a linker such as methylenebis(phosphonate), leading to mycophenolic adenine dinucleotides such as C2-MAD¹⁷ and its derivatives.¹⁸ Interestingly, C2-MAD proved resistant to glucuronidation¹⁷ probably due to the steric hindrance imposed by the additional adenosine moiety, thus making C2-MAD a poor substrate of UDP-glucuronosyltransferases.

Furthermore, as exemplified by VX-497¹⁹ and BMS-337197²⁰ (Fig. 2), structure-based drug design has yielded series of novel IMPDPH inhibitors based on a methoxy-(5-oxazolyl)-phenyl (MOP) moiety, which was believed to bind in a fashion analogous to the substituted benzofuranone present in MPA. It has been demonstrated that the oxazolyl group can form key hydrogen bonds with human IMPDPH2 residues Gly326 and Thr333, both of which also interact with the aromatic core of MPA. Nevertheless, lack of a phenolic hydroxyl group prevents VX-497 engaging in a hydrogen bonding with Thr333. Medicinal chemistry campaigns by a number of pharmaceutical companies led to numerous and structurally diverse IMPDPH inhibitors, which have been recently reviewed.³

2. Results and discussion

In our continuing efforts on the design, synthesis and evaluation of potential anti-cancer agents, we became interested in MPA derivatives and analogs devoid of the metabolically labile phenolic hydroxyl group. Here we report a series of hybrid compounds (Fig. 3, 1–4) in which a MOP moiety is connected to a hexenoic side chain. We expected that the MOP group would interact with IMPDPH as proposed for VX-497 while the hexenoic side chain would behave like that of MPA. We were interested in investigating the structure–activity relationship (SAR) of compounds in which the position of side chain is varied in relation to the MOP group. In addition, we also hoped to assess the role of methoxy and methyl groups which are placed adjacent to the side chain, as proposed in compound 3 and 4.

2.1. Chemistry

Various synthetic approaches have been devised for the synthesis of MPA and its analogs. Many of these syntheses involve formation of the aromatic moiety followed by introduction of the side chain through various methodologies such as Stille coupling,²¹ *ortho*-ester Claisen rearrangement,^{15,16} and Heck carbonylation and olefination.²² Nevertheless, a ring annulation sequence has also been proposed for the formation of aromatic ring after intro-

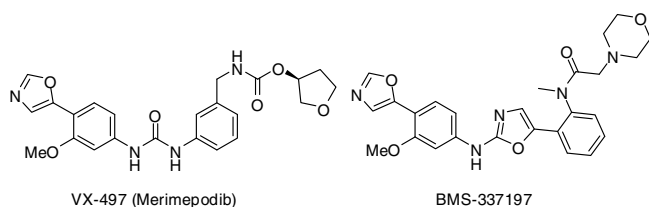


Figure 2. Representative IMPDPH inhibitors.

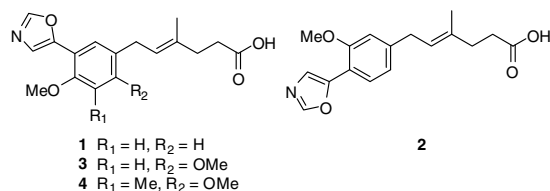


Figure 3. Mycophenolic acid analogs as IMPDPH inhibitors.

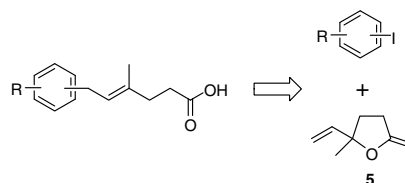
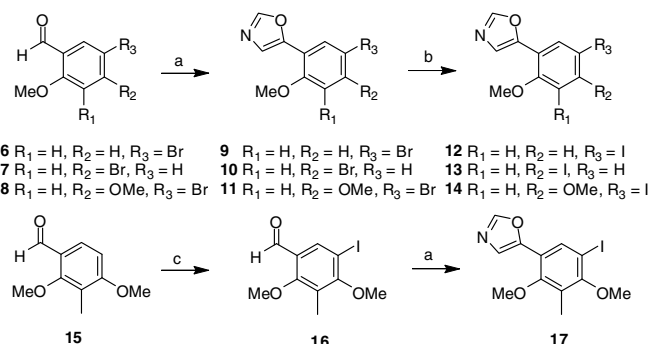


Figure 4. Retrosynthetic scheme of mycophenolic acid analogs.

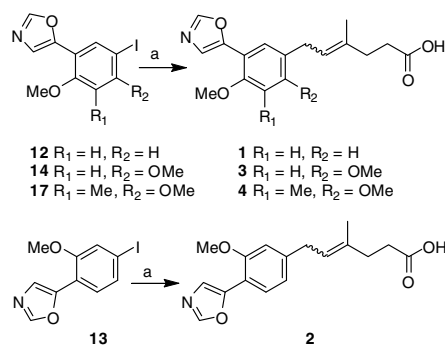
duction of the side chain.²³ For the synthesis of compounds 1–4, we devised a convergent and efficient synthetic scheme (Fig. 4), involving an allylic substitution reaction between cuprates derived from aromatic iodides and lactone 5,²⁴ which can be conveniently prepared in one step from ethyl levulinate. In our approach, the lactone serves as a leaving group and an allylic substitution reaction leads to the requisite hexenoic carboxylic acid side chain in one step. It was clear that our synthetic approach would yield a mixture of *E* and *Z* isomers. However, we assumed that the *E/Z* ratio would be similar in all the target compounds, allowing us to perform a preliminary SAR analysis. In addition, subsequent separation and evaluation individual isomers would enable us to investigate the role of olefin geometry on the inhibitory activity of pure isomers.

The syntheses of various iodides are depicted in Scheme 1. Condensation of tosylmethyl isocyanide (TosMIC) with aldehyde 6 afforded 5-oxazolyl substituted bromide 9. The conversion of bromide 9 into iodide 12 was accomplished by Buchwald's copper-catalyzed halogen exchange reaction²⁵ in excellent yields. Preparation of iodides 13 and 14 was accomplished in procedures almost identical to those described for iodide 12 from bromide 7 and 8, respectively. Finally, iodination of tetra-substituted aldehyde 15 yielded iodide 16, which was condensed with TosMIC to give iodide 17.

These iodides were converted into Grignard reagents using procedures reported by Knochel (Scheme 2).²⁶ Subsequent one-pot transmetalation gave cuprates, which underwent an allylic substitution reaction to give MPA analogs 1–4 in moderate yields.



Scheme 1. Reagents and conditions: (a) TosMIC, K₂CO₃, MeOH, reflux; (b) NaI, CuI, *trans*-*N,N*-dimethylcyclohexane-1,2-diamine, 1,4-dioxane, 110 °C; (c) I₂, silver trifluoroacetate, CHCl₃, rt.



Scheme 2. Reagents and conditions: (a) i -PrMgCl, LiCl, THF; (ii) CuBr·Me₂S, -30 °C; (iii) compound **5**, -30 °C.

As we anticipated, MPA analogs **1–4** were obtained as a mixture of *E* and *Z* isomers (Table 1). As detailed below, pure isomers of compound **3** were separated by high-performance liquid chromatography (HPLC) and hence the *E/Z* ratio was determined with *E* isomer slightly preferred over *Z* isomer. Since the final iodides as shown in Scheme 1 were structurally similar, it is reasonable to believe that compounds **1–4**, which were prepared under nearly identical reaction conditions, would show a similar selectivity toward *E* isomers.

The *E/Z* ratios as shown in Table 1 were determined based on the integrations of ¹H NMR signals displayed by individual isomers, assuming that *E* isomer was preferred. For compounds **1** and **2**, the methyl protons from the hexenoic side chain were used. However, signals from the aromatic region were used for compounds **3** and **4** since signals from the side chain methyl group were identical for both *E* and *Z* isomers. As listed in Table 1, compound **1** possessed an *E/Z* ratio of 1.5:1 while compounds **2** and **3** displayed very similar *E/Z* ratios, which would allow for a preliminary SAR analysis without separation of individual isomers. Nevertheless, compound **4** exhibited a slightly higher *E/Z* ratio.

2.2. Biological evaluations

MPA analogs **1–4** were tested against human IMPDH type 1 and type 2 (Table 1). Compound **1** showed modest activities against both type 1 and type 2. Compound **2** was approximately twofold less active than compound **1**, indicating the importance of side chain position.

Compounds **3** and **4** were designed to assess the roles played by a methoxy or methyl group which were placed adjacent to the hexenoic side chain. In MPA, the methoxy and methyl groups play crucial roles in the optimal orientation of the hexenoic side chain and therefore the high potency of MPA. For instance, the introduction of methoxy or methyl group resulted in a 280- and 20-fold increase in potency, respectively.²⁷ However, in our series of MPA analogs, attachment of a methoxy group *ortho* to the side chain in com-

pound **1** led to inhibitor **3** ($K_i = 4.3 \mu\text{M}$) which exhibited slightly enhanced potency. An additional methyl group as shown in compound **4** abrogated the inhibitory activity. This finding is clearly in contrast to the trends observed for MPA.²⁷

In order to further investigate the significance of olefin geometry, compound **3** was separated by HPLC to give compound **3-E** and **3-Z**. The olefin geometry assignment was based on the 1D nuclear overhauser effect (NOE) experiment conducted on both compound **3-E** and **3-Z**. The selective NOE interactions are shown in Figure 5. Among the NOE correlations, the most informative observation was that the vinylic proton showed a correlation with the methyl protons in **3-Z** whereas there was no such correlation observed in **3-E**. The assignment of **3-E** and **3-Z** isomers also aided the determination of *E/Z* ratio of compound **3** as shown in Table 1. Both compounds were also evaluated for their ability to inhibit human IMPDH enzymes. Isomer **3-E** ($K_i = 2.3 \mu\text{M}$) was approximately 10-fold more potent than **3-Z**, indicating the key role played by the olefin geometry in relation to IMPDH inhibition.

As indicated in Table 1, MPA analogs, like MPA itself, exhibited a slight selectivity toward IMPDH2 over IMPDH1. This observation appears to support our rationale that MPA analogs **1–4** interact with IMPDH enzymes in a mode analogous to that MPA. Interestingly, **3-E** and **3-Z** display a similar selectivity against IMPDH2, suggesting that the selectivity mainly arises from the MOP moiety whereas the geometry of side chain plays a minor role.

MPA analogs **1–3**, **3-E**, and **3-Z** were also tested for their abilities to inhibit the growth of K562 cells (Table 1) as previously described.¹⁸ In line with their modest inhibitory activity in the enzymatic assay, MPA analogs showed weak inhibition of K562 cells. Nevertheless, compounds **1–3**, **3-E**, and **3-Z** do offer an advantage considering the ratio of K562 cells proliferation IC₅₀ over IMPDH2 K_i . For instance, the ratio for compound **3** was approximately 10 and significantly lower than that of MPA (770). Given the lack of C7-hydroxyl group in our MPA analogs, it is reasonable to speculate that removal of the glucuronidation-prone hydroxyl group diminishes their metabolic liability and therefore enhances their cellular activity in comparison to their enzymatic IC₅₀ values. It was also interesting to note that compound **3-E** exhibited an inhibitory activity comparable to that of compound **3-Z** even though the former compound was approximately 10-fold more potent as an IMPDH inhibitor.

2.3. Computational modeling

On the basis of structural information available in the literature,¹⁹ the oxazole ring of MOP moiety was initially positioned within hydrogen bonding range of Gly326 and Thr333 and minimized with the OPLS-2005 forcefield in a model of the IMPDH binding site. While the measured distances and resulting geometry were reasonable, the lowest energy conformations routinely featured a Thr333 hydrogen bond to Cys331 rather than the expected interaction with the ligand. To determine the accuracy of the forcefield model, the structure was re-minimized using a hybrid QM/MM method. That is, while most of the receptor was modeled with the OPLS-2005 forcefield (all residues within five angstroms of the

Table 1
^a*E/Z* ratios and biological evaluations of MPA analogs

| Compound | <i>E/Z</i> ratio | IMPDH1 K_i (μM) | IMPDH2 K_i (μM) | K562 cells proliferation IC ₅₀ (μM) |
|------------|------------------|--------------------------------|--------------------------------|---|
| MPA | NA | 0.04 | 0.01 | 7.7 |
| 1 | 1.5:1 | 20.8 ± 1.4 | 8.7 ± 1.0 | >100 |
| 2 | 1.5:1 | 42.8 ± 3.2 | 14.3 ± 1.8 | >100 |
| 3 | 1.9:1 | 16.0 ± 2.4 | 4.3 ± 0.5 | 56 |
| 4 | 2.8:1 | >100 | >100 | ND |
| 3-E | NA | 10.3 ± 1.2 | 2.3 ± 0.2 | 88 |
| 3-Z | NA | 97.3 ± 33.9 | 30.1 ± 3.3 | 71 |

^a NA, not applicable; ND, not determined.

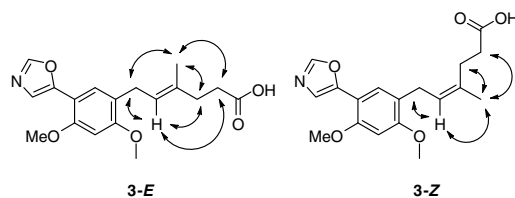


Figure 5. NOE correlations observed for compound **3-E** and **3-Z**.

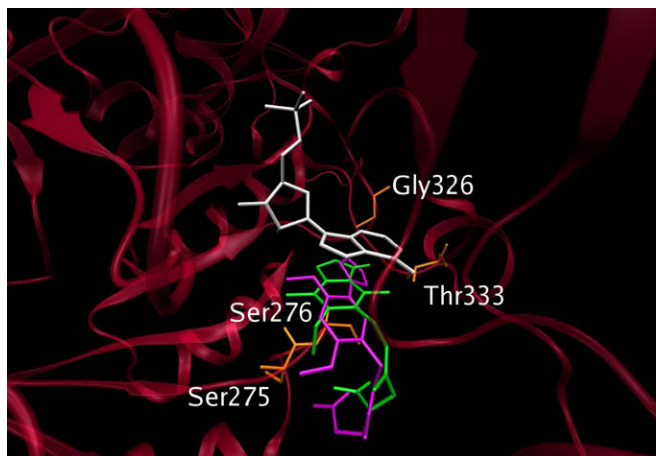


Figure 6. Compound **3-E** is overlaid with MPA in the IMPDH crystal structure 1JR1. The protein is presented in red ribbon while MPA and **3-E** are green and mauve sticks, respectively. Key residues are shown as orange sticks. The nucleotide substrate is colored white.

ligand allowed to move), the ligand and several important residues (Thr333, Ser275, and Ser276) were treated at the B3LYP/6-31G* level of theory which yielded the conformation presented in Figure 6. A hydrogen bond between Thr333 and the ring oxygen is present (3.2 angstroms, 169 degrees) as expected. Moreover, MPA is superimposed on **3-E** as shown in Figure 6. The reduced potency of compound **1** relative to **2** can be explained by the position to which the hexenoic acid chain is attached to MOP. Attachment at the *meta*-position leads to an inhibitor that closely mimics MPA, superior to attachment at the *para*-position.

However, a significant loss in activity is observed in compound **3-E** with respect to MPA even though the acid tail is attached *meta* to the oxazole ring. Furthermore, addition of a methyl group at the position that is *ortho* to both methoxy groups in **3** results in **4**, an inactive compound. The complete lack of activity is initially surprising as this region of the protein is apparently devoid of steric and electrostatic clashes with the methyl group. Instead, the effect appears to be due to the methyl group's influence on the ligand itself and subtle changes in the conformation of the hexenoic chain that reduce binding affinity. In both cases it seems that MOP, while a reasonable replacement for the MPA benzofuranone head group, is not the best choice for pairing with the hexenoic acid tail. Qualitatively this observation can be demonstrated by the relatively different position and conformation of the chain in Figure 6. The sensitivity of IMPDH to changes in the tail is well documented,²⁸ and it has been suggested that the loss in potency due to modifications of the acid tail is related to a weakening of its interaction with Ser276.¹⁹ The carboxylic acid forms at least two hydrogen bonds (Ser276 side chain and backbone). Using the QM/MM treatment described above interaction energies can be calculated for the ligand–receptor complexes. The ligand is optimized in both a receptor and solvent environment and the relative interaction is evaluated according to the following equation:

$$E(I) = E(\text{complex}) - [E(\text{receptor}) + E(\text{ligand})].$$

While we stress that much of the thermodynamic cycle is missing from a simple end point analysis, the general trend of MPA (–208 kcal/mol) > **3-E** (–181 kcal/mol) > **4-E** (–131 kcal/mol) correlates well with their inhibitory activities in enzymatic assays. As the conformations examined of each molecule maintain the appropriate hydrogen bonding with Ser276, it further suggests that subtle conformational shifts are indeed enough to significantly alter the binding free energy and therefore provides an explanation in agreement with the observed SAR.

3. Conclusions

In summary, we have designed a series of MPA analogs devoid of the metabolically labile C7-hydroxyl group based on the combination of structural elements from MPA and IMPDH inhibitors previously reported. We have devised a convergent synthetic scheme which allowed a rapid assembly of our target compounds from substituted aromatic iodides and lactone **5**. Through these studies, we have demonstrated that replacement of the benzofuranone moiety of MPA by a MOP group retains biological activities. The resulting MPA analogs displayed modest activity against isoforms of human IMPDH and weak activity against K562 cells. We have also observed an enhancement of cellular activity in our MPA analogs in comparison to their enzymatic potency, presumably because these MPA analogs are not susceptible to glucuronidation which has severely limited MPAs medical applications. Further studies on metabolically stable MPA analogs are currently in progress.

4. Experimental

4.1. General methods

All commercial reagents (Sigma–Aldrich, Acros) were used as provided unless otherwise indicated. An anhydrous solvent dispensing system (J.C. Meyer) using 2 packed columns of neutral alumina was used for drying THF, Et₂O, and CH₂Cl₂, while 2 packed columns of molecular sieves were used to dry DMF. Solvents were dispensed under argon. Flash chromatography was performed with Ultra Pure silica gel (Silicycle) with the indicated solvent system. Nuclear magnetic resonance spectra were recorded on a Varian 600 MHz with Me₄Si or signals from residual solvent as the internal standard for ¹H or ¹³C. Chemical shifts are reported in ppm, and signals are described as s (singlet), d (doublet), t (triplet), q (quartet), m (multiplet), br s (broad singlet), and dd (doublet). Values given for coupling constants are first order. The *E/Z* ratios were determined based on the integrations of ¹H NMR signals displayed by individual isomers. High resolution mass spectra were recorded on an Agilent TOF II TOF/MS instrument equipped with either an ESI or APCI interface.

4.2. Chemical synthesis

4.2.1. Bromide **9**

A mixture of commercially available 5-bromo-2-methoxybenzaldehyde (**6**, 2.28 g, 10.6 mmol), tosylmethyl isocyanide (TosMIC, 2.09 g, 10.6 mmol) and K₂CO₃ (3.72 g, 26.9 mmol) in anhydrous MeOH (30 mL) was heated at reflux for 22 h. After cooling to rt, the mixture was poured into 300 mL of ice-water and the solid precipitated was filtered. The solid was washed with water, air-dried, collected and dried in vacuo to give bromide **9** as a yellow solid (2.59 g, 96%). ¹H NMR (CDCl₃) δ 7.91 (s, 1H), 7.89 (d, *J* = 2.4 Hz, 1H), 7.57 (s, 1H), 7.39 (dd, *J* = 8.4, 2.4 Hz, 1H), 6.86 (d, *J* = 8.4 Hz, 1H), 3.95 (s, 3H). ¹³C NMR (CDCl₃) δ 154.6, 149.8, 146.6, 131.6, 128.6, 126.4, 118.8, 113.2, 112.6, 55.8. MS (ESI) calcd for C₁₀H₉BrNO₂ 254.0 (M+H)⁺, found 254.0.

4.2.2. Bromide **10**

Following procedures similar to those described for bromide **9**, commercially available 4-bromo-2-methoxybenzaldehyde (**7**, 1.40 g, 6.53 mmol) was converted into bromide **10** as a yellowish solid (1.56 g, 94%). ¹H NMR (CDCl₃) δ 7.90 (s, 1H), 7.63 (d, *J* = 8.4 Hz, 1H), 7.54 (s, 1H), 7.19 (d, *J* = 8.4 Hz, 1H), 7.12 (s, 1H), 3.96 (s, 3H). ¹³C NMR (CDCl₃) δ 156.0, 149.6, 147.2, 127.0, 125.8, 124.0, 122.6, 116.2, 114.6, 55.8. MS (ESI) calcd for C₁₀H₉BrNO₂ 254.0 (M+H)⁺, found 254.0.

4.2.3. Bromide 11

Following procedures similar to those described for bromide **9**, commercially available 5-bromo-2,4-dimethoxybenzaldehyde (**8**, 5.08 g, 20.7 mmol) was converted into bromide **11** as a yellow solid (5.60 g, 95%). ¹H NMR (CDCl₃) δ 7.84 (s, 1H), 7.79 (s, 1H), 7.36 (s, 1H), 6.46 (s, 1H), 3.90 (s, 3H), 3.87 (s, 3H). ¹³C NMR (CDCl₃) δ 156.5, 156.2, 149.2, 146.8, 129.9, 124.3, 111.3, 102.5, 96.2, 56.4, 55.8. MS (ESI) calcd for C₁₁H₁₁BrNO₂ 284.0 (M+H)⁺, found 284.0.

4.2.4. Iodide 12

A mixture of bromide **9** (1.52 g, 6.00 mmol), CuI (59 mg, 0.31 mmol), and NaI (1.81 g, 12.1 mmol) in anhydrous 1,4-dioxane (6.0 mL) was evacuated and backfilled with N₂ for five times. After addition of racemic *trans*-*N,N'*-dimethylcyclohexane-1,2-diamine (95 μL, 0.60 mmol), the mixture was heated at 110 °C for 24 h and then cooled to rt. The mixture was poured into 200 mL of ice-water and the solid precipitated was filtered. The solid was washed with water, air-dried, collected and then dried in vacuo to give iodide **12** as a slightly tan solid (1.77 g, 98%). ¹H NMR (CDCl₃) δ 8.07 (d, *J* = 2.4 Hz, 1H), 7.91 (s, 1H), 7.62–7.50 (m, 2H), 6.75 (d, *J* = 9.0 Hz, 1H), 3.95 (s, 3H). ¹³C NMR (CDCl₃) δ 155.4, 137.7, 134.4, 119.2, 113.1, 82.9, 67.1, 55.6. MS (ESI) calcd for C₁₀H₉INO₂ 302.0 (M+H)⁺, found 302.0.

4.2.5. Iodide 13

Following procedures similar to those described for iodide **12**, bromide **10** (1.36 g, 5.35 mmol) was converted into iodide **13** as a slightly tan solid (1.56 g, 97%). ¹H NMR (CDCl₃) δ 7.92 (s, 1H), 7.56 (s, 1H), 7.48 (d, *J* = 7.8 Hz, 1H), 7.40 (d, *J* = 8.4 Hz, 1H), 7.30 (s, 1H), 3.96 (s, 3H). ¹³C NMR (CDCl₃) δ 155.8, 130.1, 127.2, 120.3, 116.8, 93.9, 67.1, 55.8. MS (ESI) calcd for C₁₀H₉INO₂ 302.0 (M+H)⁺, found 302.0.

4.2.6. Iodide 14

Following procedures similar to those described for iodide **12**, bromide **11** (3.41 g, 12.0 mmol) was converted into iodide **14** as a slightly tan solid (3.64 g, 92%). ¹H NMR (CDCl₃) δ 8.05 (s, 1H), 7.80 (s, 1H), 7.36 (s, 1H), 6.41 (s, 1H), 3.90 (s, 3H), 3.86 (s, 3H). ¹³C NMR (CDCl₃) δ 158.9, 157.3, 149.2, 146.7, 135.8, 124.2, 112.1, 95.4, 74.7, 56.5, 55.7. MS (ESI) calcd for C₁₁H₁₁INO₃ 332.0 (M+H)⁺, found 332.0.

4.2.7. Iodide 16

To a mixture of commercially available 2,4-dimethoxy-3-methylbenzaldehyde (**15**, 3.13 g, 17.4 mmol) and silver trifluoroacetate (4.60 g, 20.8 mmol) was added a solution of iodine (5.30 g, 20.9 mmol) in CHCl₃ (200 mL). After the addition was complete, the mixture was allowed to stir for 4 h. Additional silver trifluoroacetate (770 mg, 3.48 mmol) and iodine (880 mg, 3.47 mmol) were added and the mixture was allowed to stir overnight. The reaction mixture was filtered through a pad of Celite, and the filtrate was washed with saturated NaHCO₃ (200 mL), a solution of Na₂S₂O₃ (200 mL), water (2 × 200 mL) and brine (200 mL). The organic layer was dried over Na₂SO₄ and then filtered. The filtrate was concentrated and dried in vacuo to give iodide **16** as a pale solid (5.10 g, 96%). ¹H NMR (CDCl₃) δ 10.19 (s, 1H), 8.14 (s, 1H), 3.88 (s, 3H), 3.83 (s, 3H), 2.32 (s, 3H). ¹³C NMR (CDCl₃) δ 188.1, 164.0, 163.4, 136.6, 127.3, 127.2, 87.0, 63.4, 60.5, 10.1. MS (ESI) calcd for C₁₀H₁₂IO₃ 307.0 (M+H)⁺, found 307.0.

4.2.8. Iodide 17

A mixture of iodide **16** (3.58 g, 11.7 mmol), TosMIC (2.33 g, 11.9 mmol) and K₂CO₃ (4.05 g, 29.3 mmol) in anhydrous MeOH (60 mL) was heated at reflux for 24 h. After cooling to rt, the mixture was poured into 500 mL of ice-water and the solid precipitated was filtered. The solid was washed with water, air-dried,

collected and dried in vacuo to give iodide **17** as a pale solid (3.74 g, 93%). ¹H NMR (CDCl₃) δ 8.03 (s, 1H), 7.91 (s, 1H), 7.55 (s, 1H), 3.80 (s, 3H), 3.73 (s, 3H), 2.34 (s, 3H). ¹³C NMR (CDCl₃) δ 159.1, 156.5, 149.9, 146.6, 133.3, 126.9, 125.0, 119.9, 86.4, 60.4, 59.7, 10.5. MS (ESI) calcd for C₁₂H₁₃INO₃ 346.0 (M+H)⁺, found 346.1.

4.2.9. Carboxylic acid 1

To dry THF (30 mL) at –30 °C were added a solution of ¹PrMgCl (1.4 M in THF, 3.0 mL, 4.2 mmol) and LiCl (184 mg, 4.34 mmol) and the mixture was allowed to stir for 30 min. After addition of iodide **12** (906 mg, 3.01 mmol), the resulting solution was allowed to stir at –30 °C for 2 h and CuBr·Me₂S (869 mg, 4.22 mmol) was added. After stirring for 1 h, a solution of lactone **5**²⁴ (255 mg, 2.02 mmol) in dry THF (3 mL) was added and the resulting mixture was allowed to stir at –30 °C for 18 h. The reaction mixture was poured into saturated NH₄Cl (200 mL plus 10 mL of 1 N HCl) and the mixture was extracted with EtOAc (200 mL). The organic layer was washed with brine (2 × 100 mL) and then dried over MgSO₄. After filtration, the filtrate was concentrated and the residue was purified by column chromatography (1–9% MeOH/CH₂Cl₂) to give carboxylic acid **1** (*E/Z* ratio ≈ 1.5:1) as a greenish syrup (127 mg, 21%). ¹H NMR (CDOD₃) δ 8.28 (s, 1H), 7.72–7.44 (m, 2H), 7.12 (d, *J* = 6.6 Hz, 1H), 6.99 (d, *J* = 8.4 Hz, 1H), 5.42–5.32 (m, 1H), 3.92 (s, 3H), 3.38–3.32 (m, 2H), 2.47 (br s, 2H), 2.35 (br s, 2H), 1.75 (s, 1.2H), 1.75 (s, 1.8H). HRMS calcd for C₁₇H₁₈NO₄ 300.1235 (M–H)[–], found 300.1237.

4.2.10. Carboxylic acid 2

Following procedures similar to those described for carboxylic acid **1**, iodide **13** (452 mg, 1.50 mmol) and lactone **5** (128 mg, 1.01 mmol) underwent an allylic substitution to give carboxylic acid **2** (*E/Z* ratio ≈ 1.5:1) as a greenish syrup (107 mg, 35%). ¹H NMR (CDOD₃) δ 8.32 (br s, 1H), 7.90–7.50 (m, 2H), 6.96–6.74 (m, 2H), 5.45–5.32 (m, 1H), 3.93 (s, 3H), 3.44–3.34 (m, 2H), 2.62–2.32 (m, 4H), 1.74 (s, 1.2H), 1.73 (s, 1.8H). HRMS calcd for C₁₇H₁₈NO₄ 300.1235 (M–H)[–], found 300.1238.

4.2.11. Carboxylic acid 3

Following procedures similar to those described for carboxylic acid **1**, iodide **14** (1.50 g, 4.53 mmol) and lactone **5** (382 mg, 3.03 mmol) underwent an allylic substitution to give carboxylic acid **3** (*E/Z* ratio ≈ 1.9:1) as a greenish syrup (404 mg, 40%). ¹H NMR (CDOD₃) δ 8.18 (br s, 1H), 7.47 (s, 0.3H), 7.46 (s, 0.7H), 7.42 (s, 1H), 6.66 (s, 1H), 5.38–5.28 (m, 1H), 3.96 (s, 3H), 3.88 (s, 3H), 3.29–3.23 (m, 2H), 2.50–2.28 (m, 4H), 1.72 (s, 3H). MS (ESI) calcd for C₁₈H₂₀NO₅ 330.1 (M–H)[–], found 330.1.

4.2.12. Carboxylic acid 4

Following procedures similar to those described for carboxylic acid **1**, iodide **17** (1.03 g, 2.99 mmol) and lactone **5** (378 mg, 3.00 mmol) underwent an allylic substitution to give carboxylic acid **4** (*E/Z* ratio ≈ 2.8:1) as a clear syrup (478 mg, 46%). ¹H NMR (CDCl₃) δ 7.94 (s, 0.25H), 7.94 (s, 0.75H), 7.53 (s, 0.25H), 7.52 (s, 0.75H), 7.39 (s, 0.75H), 7.38 (s, 0.25H), 5.40–5.33 (m, 1H), 3.75 (s, 2.2H), 3.74 (s, 0.8H), 3.71 (s, 3H), 3.42–3.36 (m, 2H), 2.56–2.46 (m, 3H), 2.42–2.36 (m, 1H), 2.28 (s, 3H), 1.77 (s, 3H). HRMS calcd for C₁₉H₂₂NO₅ 344.1503 (M–H)[–], found 344.1516.

4.2.13. HPLC separation of *E/Z* isomers of carboxylic acid 3

The analytical HPLC was performed on a Varian Microsorb column (C18, 5 μ, 4.6 × 250 mm) with a flow rate of 0.5 mL/min while the preparative HPLC was performed on a Varian Dynamax column (C18, 8 μ, 41.4 × 250 mm) with a flow rate of 40 mL/min. An isocratic (21%) gradient of CH₃CN (with 0.1% Et₃N) in water (with 1% Et₃N) was used. Combined fractions were pooled and the organ-

ic solvent was removed. The aqueous layer (with a reduce volume) was acidified with 1 N HCl to pH \approx 3. The individual solid precipitate was filtered, washed with water, air-dried and dried in vacuo to give carboxylic acid **3-Z** (retention time = 9.6 min) and **3-E** (retention time = 12 min).

4.2.13.1. Carboxylic acid 3-E. $^1\text{H NMR}$ (CDCl_3) δ 7.86 (s, 1H), 7.48 (s, 1H), 7.41 (s, 1H), 6.50 (s, 1H), 5.37 (t, $J = 7.2$ Hz, 1H), 3.95 (s, 3H), 3.88 (s, 3H), 3.30 (d, $J = 7.2$ Hz, 2H), 2.49 (t, $J = 7.8$ Hz, 2H), 2.37 (t, $J = 7.5$ Hz, 2H), 1.74 (s, 3H). $^{13}\text{C NMR}$ ($\text{CD}_3\text{OD}/\text{CDCl}_3$) δ 177.3, 160.0, 157.0, 150.8, 150.1, 135.7, 127.4, 124.4, 123.3, 123.1, 109.8, 96.2, 56.3, 56.2, 35.8, 34.0, 28.7, 16.3. HRMS calcd for $\text{C}_{18}\text{H}_{20}\text{NO}_5$ 330.1335 ($\text{M}-\text{H}$) $^-$, found 330.1355.

4.2.13.2. Carboxylic acid 3-Z. $^1\text{H NMR}$ (CDCl_3) δ 7.87 (s, 1H), 7.50 (s, 1H), 7.41 (s, 1H), 6.50 (s, 1H), 5.36 (t, $J = 7.2$ Hz, 1H), 3.95 (s, 3H), 3.88 (s, 3H), 3.32 (d, $J = 7.2$ Hz, 2H), 2.51 (t, $J = 7.2$ Hz, 2H), 2.47 (t, $J = 7.2$ Hz, 2H), 1.75 (s, 3H). $^{13}\text{C NMR}$ (CD_3OD) δ 177.5, 160.2, 157.2, 151.2, 150.3, 135.8, 127.6, 125.8, 123.4, 123.4, 110.0, 96.5, 56.3, 56.2, 34.0, 28.6, 28.4, 23.4. HRMS calcd for $\text{C}_{18}\text{H}_{20}\text{NO}_5$ 330.1335 ($\text{M}-\text{H}$) $^-$, found 330.1354.

4.3. Enzyme assays

IMPDH inhibition assays were performed essentially as described.²⁹ Briefly, assays were set up in duplicate and contained either IMPDH type 1 (100 nM) or type 2 (30 nM) in reaction buffer (50 mM Tris, pH 8.0, 100 mM KCl, 1 mM DTT, 100 μM IMP, and 100 μM NAD). Inhibitors in DMSO were added to UV clear 96-well half-area plates (Greiner) to give a final DMSO concentration of 1%. One hundred microliters of the reaction mixture was dispensed into the plates immediately after the addition of enzyme. Reactions were run at 25 $^\circ\text{C}$ and the production of NADH was monitored by following changes in absorbance at 340 nm on a Molecular Devices M5e multimode plate reader. Steady state velocities were used to determine IC_{50} and K_i^{APP} values by fitting the velocities versus inhibitor concentration to the sigmoidal concentration-response curve (variable slope) and the Morrison equation,³⁰ respectively, using GraphPad Prism. For more accurate K_i^{APP} values when the Morrison equation was used, enzyme concentration was fixed using the specific activities of IMPDH I and II, 0.12 and 0.35 $\mu\text{mol}/(\text{min mg})$, respectively.

4.4. Molecular modeling

Model construction has been described elsewhere.¹⁸ All calculations were completed with the Schrodinger computational chemistry software which includes MacroModel³¹ for molecular mechanics and Qsite³² for quantum mechanics. The ligands were initially built utilizing structural information from multiple sources^{19,33} and subjected to a conformational search using MacroModel and the OPLS forcefield.^{34,35} After 10,000 steps that probed translations of the ligand as well as sampled all rotatable bonds the global minimum and vast majority of conformations within 5.0 kcal/mol maintained the hexenoic acid tail hydrogen bonding with Ser276. The global minimum was further optimized at the B3LYP^{36,37}/6-31G^{*38} level of theory and subject to the interaction energy calculation as described.

Acknowledgments

These studies were founded by the Center for Drug Design, Academic Health Center, University of Minnesota. We thank Dr. Courtney Aldrich for his help with the biological assays.

References and notes

- Bentley, R. *Chem. Rev.* **2000**, *100*, 3801.
- Chen, L.; Pankiewicz, K. W. *Curr. Opin. Drug Discov. Dev.* **2007**, *10*, 403.
- Ratcliffe, A. J. *Curr. Opin. Drug Discov. Dev.* **2006**, *9*, 595.
- Floryk, D.; Huberman, E. *Cancer Lett.* **2006**, *231*, 20.
- Floryk, D.; Tollaksen, S. L.; Giometti, C. S.; Huberman, E. *Cancer Res.* **2004**, *64*, 9049.
- Yu, J.; Lemas, V.; Page, T.; Connor, J. D.; Yu, A. L. *Cancer Res.* **1989**, *49*, 5555.
- Kiguchi, K.; Collart, F. R.; Henning-Chubb, C.; Huberman, E. *Cell Growth Differ.* **1990**, *1*, 259.
- Chong, C. R.; Qian, D. Z.; Pan, F.; Wei, Y.; Pili, R.; Sullivan, D. J., Jr.; Liu, J. O. *J. Med. Chem.* **2006**, *49*, 2677.
- Gu, J. J.; Santiago, L.; Mitchell, B. S. *Blood* **2005**, *105*, 3270.
- Ubukata, M.; Takamori, H.; Ohashi, M.; Mitsuhashi, S.; Yamashita, K.; Asada, T.; Nakajima, N.; Matsuura, N.; Tsuruga, M.; Taki, K.; Magae, J. *Bioorg. Med. Chem. Lett.* **2007**, *17*, 4767.
- Chen, L.; Wilson, D.; Jayaram, H. N.; Pankiewicz, K. W. *J. Med. Chem.* **2007**, *50*, 6685.
- Takebe, N.; Cheng, X.; Wu, S.; Bauer, K.; Goloubeva, O. G.; Fenton, R. G.; Heyman, M.; Rapoport, A. P.; Badros, A.; Shaughnessy, J.; Ross, D.; Meisenberg, B.; Tricot, G. *Clin. Cancer Res.* **2004**, *10*, 8301.
- Papageorgiou, C. *Mini-Rev. Med. Chem.* **2001**, *1*, 71.
- Franklin, T. J.; Jacobs, V. N.; Jones, G.; Ple, P. *Drug Metab. Dispos.* **1997**, *25*, 367.
- Lai, G.; Anderson, W. K. *Tetrahedron* **2000**, *56*, 2583.
- El-Araby, M. E.; Bernacki, R. J.; Makara, G. M.; Pera, P. J.; Anderson, W. K. *Bioorg. Med. Chem.* **2004**, *12*, 2867.
- Pankiewicz, K. W.; Lesiak-Watanabe, K. B.; Watanabe, K. A.; Patterson, S. E.; Jayaram, H. N.; Yalowitz, J. A.; Miller, M. D.; Seidman, M.; Majumdar, A.; Prehna, G.; Goldstein, B. M. *J. Med. Chem.* **2002**, *45*, 703.
- Chen, L.; Gao, G.; Felczak, K.; Bonnac, L.; Patterson, S. E.; Wilson, D.; Bennett, E. M.; Jayaram, H. N.; Hedstrom, L.; Pankiewicz, K. W. *J. Med. Chem.* **2007**, *50*, 5743.
- Sintchak, M. D.; Nimmesgern, E. *Immunopharmacology* **2000**, *47*, 163.
- Dhar, T. G. M.; Shen, Z. Q.; Guo, J. Q.; Liu, C. J.; Watterson, S. H.; Gu, H. H.; Pitts, W. J.; Fleener, C. A.; Rouleau, K. A.; Sherbina, N. Z.; McIntyre, K. W.; Witmer, M. R.; Tredup, J. A.; Chen, B. C.; Zhao, R. L.; Bednarz, M. S.; Cheney, D. L.; MacMaster, J. F.; Miller, L. M.; Berry, K. K.; Harper, T. W.; Barrish, J. C.; Hollenbaugh, D. L.; Iwanowicz, E. J. *J. Med. Chem.* **2002**, *45*, 2127.
- Ple, P. A.; Hamon, A.; Jones, G. *Tetrahedron* **1997**, *53*, 3395.
- Lee, Y. M.; Fujiwara, Y.; Ujita, K.; Nagatomo, M.; Ohta, H.; Shimizu, I. *Bull. Chem. Soc. Jpn.* **2001**, *74*, 1437.
- Covarrubias-Zuniga, A.; Gonzalez-Lucas, A.; Dominguez, M. M. *Tetrahedron* **2003**, *59*, 1989.
- Pope, S. A.; Burtin, G. E.; Clayton, P. T.; Madge, D. J.; Muller, D. P. *Free Radical Biol. Med.* **2002**, *33*, 807.
- Klapars, A.; Buchwald, S. L. *J. Am. Chem. Soc.* **2002**, *124*, 14844.
- Krasovskiy, A.; Knochel, P. *Angew. Chem., Int. Ed.* **2004**, *43*, 3333.
- Nelson, P. H.; Carr, S. F.; Devens, B. H.; Eugui, E. M.; Franco, F.; Gonzalez, C.; Hawley, R. C.; Loughhead, D. G.; Milan, D. J.; Papp, E.; Patterson, J. W.; Rouhafza, S.; Sjogren, E. B.; Smith, D. B.; Stephenson, R. A.; Talamas, F. X.; Waltos, A. M.; Weikert, R. J.; Wu, J. C. *J. Med. Chem.* **1996**, *39*, 4181.
- Nelson, P. H.; Eugui, E.; Wang, C. C.; Allison, A. C. *J. Med. Chem.* **1990**, *33*, 833.
- Umejiego, N. N.; Li, C.; Riera, T.; Hedstrom, L.; Striepen, B. *J. Biol. Chem.* **2004**, *279*, 40320.
- Morrison, J. F. *Biochim. Biophys. Acta* **1969**, *185*, 269.
- MacroModel. Schrodinger, LLC: New York, NY, 2006.
- Qsite, version 4.5, Schrodinger, LLC: New York, NY, 2007.
- Sintchak, M. D.; Fleming, M. A.; Futer, O.; Raybuck, S. A.; Chambers, S. P.; Caron, P. R.; Murcko, M. A.; Wilson, K. P. *Cell* **1996**, *85*, 921.
- Kaminski, G. A.; Friesner, R. A.; Tirado-Rives, J.; Jorgensen, W. L. *J. Phys. Chem. B* **2001**, *105*, 6474.
- Kaminski, G. A.; Stern, H. A.; Berne, B. J.; Friesner, R. A.; Cao, Y. X.; Murphy, R. B.; Zhou, R.; Halgren, T. A. *J. Comput. Chem.* **2002**, *23*, 1515.
- Lee, C. T.; Yang, W. T.; Parr, R. G. *Phys. Rev. B* **1988**, *37*, 785.
- Becke, A. D. *J. Chem. Phys.* **1993**, *98*, 5648.
- Ditchfield, R.; Hehre, W. J.; Pople, J. A. *J. Chem. Phys.* **1971**, *54*, 724.